

# An experimental investigation of the effects of diode laser surface hardening of AISI 410 stainless steel and comparison with furnace hardening heat treatment

**Moradi, M., Arabi, H. & Kaplan, A. F. H.**

Author post-print (accepted) deposited by Coventry University's Repository

**Original citation & hyperlink:**

Moradi, M, Arabi, H & Kaplan, AFH 2019, 'An experimental investigation of the effects of diode laser surface hardening of AISI 410 stainless steel and comparison with furnace hardening heat treatment', *Journal of the Brazilian Society of Mechanical Sciences and Engineering*, vol. 41, 434.

<https://doi.org/10.1007/s40430-019-1925-2>

DOI 10.1007/s40430-019-1925-2

ISSN 1678-5878

ESSN 1806-3691

Publisher: Springer

*The final publication is available at Springer via <http://dx.doi.org/10.1007/s40430-019-1925-2>*

**Copyright © and Moral Rights are retained by the author(s) and/ or other copyright owners. A copy can be downloaded for personal non-commercial research or study, without prior permission or charge. This item cannot be reproduced or quoted extensively from without first obtaining permission in writing from the copyright holder(s). The content must not be changed in any way or sold commercially in any format or medium without the formal permission of the copyright holders.**

**This document is the author's post-print version, incorporating any revisions agreed during the peer-review process. Some differences between the published version and this version may remain and you are advised to consult the published version if you wish to cite from it.**

# **An experimental investigation of the effects of diode laser surface hardening of AISI 410 stainless steel and comparison with furnace hardening heat treatment**

**Mahmoud Moradi<sup>1,2\*</sup>, Hossein Arabi<sup>1,2</sup>, Alexander F.H. Kaplan<sup>3</sup>**

1- Department of Mechanical Engineering, Faculty of Engineering, Malayer University, P.O. Box 65719-95863 Malayer, Iran

2- Laser Materials Processing Research Centre, Malayer University, Malayer, Iran.

3- Department of Engineering Sciences and Mathematics, Lulea University of Technology, 971 87, Lulea, Sweden

Email: <sup>1</sup>moradi.malayeru@gmail.com, <sup>2</sup>arabi8252@gmail.com, <sup>3</sup> alexander.kaplan@ltu.se

## **Abstract**

This study investigated the ability of the continuous wave diode laser surface hardening on AISI 410 martensitic stainless steel with a maximum power of 1600 W. Variable process parameters; scanning speed (4-7 mm/s), laser power (1200-1600 Watts) and stand-off distance (65-75mm) were considered in this study. Micro-hardness, the geometry of hardened layer (depth and width), micro-hardness deviation from the base metal micro-hardness (MHD), microstructure analysis of the laser-hardened zone through optical microscopy (OM) and field emission scanning electron microscopy (FE-SEM) and percentage of the ferrite phase in AISI 410 microstructure by using clemex software were considered as process output responses. Results confirmed that by increasing the laser power and reducing the scanning speed, the surface hardness and depth of hardness increase. It is also revealed the width of the hardened area increases by enhancing in stand-off distance and reduction the laser power. Maximum hardness of 630 HV0.3 with 2.2 mm depth is obtained. Also, the furnace hardening heat treatment compared with the laser hardening process. Microstructure, microhardness, and impact test of the two processes are compared. Results showed that the hardness of the diode laser is 1.4 times the hardness of the furnace hardening heat treatment.

**Keywords:** Laser surface hardening; Diode laser; Microhardness; AISI410 martensitic stainless steel; Microhardness deviation.

## 1. Introduction

To improve surface properties of materials, especially steels, which are widely used in industry, traditional heat treatment methods are very popular, but modern methods like laser surface treatment are more precise [1]. Laser processing is used for various applications such as laser welding, brazing, and hardening [2-7], laser drilling [8], and laser cutting [9]. The diode lasers are one of the most used and advanced lasers in the modern industry. This type of laser with high accuracy heat-treated the surface of the matter. Martensitic stainless steels are used in several industries including petroleum, gas and petrochemical, food and pharmaceutical. These alloys are used in manufacturing corrosion resistance pipes and plates and applied in an acidic environment which are more economical than similar grades [10]. One type of martensitic stainless steels widely used in industry is AISI 410 from 400 series of these steels. Surface hardening is one of the laser surface treatment processes in which the laser is selected with preset parameters. These parameters are variables depends on the type of laser and material to be treated. After selecting optimum parameters, laser hardening accomplishes, and surface hardness of steel improves which transformation of ferrite and austenite phase to martensite will lead to more hardness [11]. Mahmoodi et al. [12] carried out laser surface treatment of AISI 420 by means of Nd:YAG laser in pulsed module, which in their research micro-hardness in depth and width of hardened area were studied. To compare the ability of CO<sub>2</sub> laser and diode laser in hardening of AISI 1045, Li et al. [13] investigated the effect of each process on quality of the surface hardening. According to experimental data of laser hardening by these two types of lasers, they simulated the process, which showed the quality achieved by high power diode laser was higher than the one by CO<sub>2</sub> laser. Guarino et al. [14] were used a high-power diode laser to develop the fatigue life of AISI 1040 steel. Results revealed that laser treatment could considerably increase the fatigue life. Netprasert et al. [15] studied to harden the AISI 420 martensitic stainless steel by using a nanosecond pulse laser. The results showed that the micro-hardness increased from 242 HV to 1700 HV and depth of the hardened layer was created to be 60-80  $\mu\text{m}$ . Yazici et al. [16] investigated the effect of different processing temperatures on wear properties of high power diode laser on R260 grade rail steel. Martinez et al. [17] surveyed the effects of the distinctly applied laser heat treatment (LHT) and ultrasonic impact treatment (UIT) and the joined LHT + UIT process on the wear and friction behaviors of the hardened surface layers of the tool steel AISI D2. Syed et al. [18] studied effects of surface hardening by using a high power

diode laser. On C-Mn low carbon automotive steel. N. Barka et al. [19] were Investigated a simulating model (finite difference method) and experimental method for laser hardening of 4340 steel. Telasang et al. [20] were investigated properties of corrosion resistance and wear of AISI H13 steel, which hardened up to 800 Vickers. Fahdil Idan et al. [21] compared the effects of CO2 laser hardening and tempering of 40, 40Cr and 38Cr2MoAl steels in GOST Russian standard. Saftar et al. [22] investigated the effects of beam geometries (circular, inverse triangle, rectangular beams) by using high power diode laser on the laser surface hardening process. Moradi et al. [23] studied on laser surface hardening of AISI 410 by using a 700 watts Nd:YAG laser in which the effect of laser pulse energy and focal point position on geometrical dimensions and microhardness of hardened zone was investigated. Jahromi et al. [24] investigated a study by Nd:YAG laser on the three different microstructures of AISI 410 martensitic stainless steel samples were heat treated including: fine ferrite, fine and coarse martensite. Furthermore, finite element simulation was done using ABAQUS software to predict diffusion on the hardness of the different microstructures by using Nd:YAG laser. A mathematical model for Nd:YAG laser surface hardening of 42CrMo steel was presented by using finite element method and verified by experimental results by sun et al. [25]. Ehlers et al. [26] carried out laser surface hardening of AISI 4140 steel sheet by using a 2000W diode laser. The maximum hardness reached to 740 HV with 1.9 mm depth in this study.

In spite of the efforts of these and other researchers, investigation on diode laser hardening of AISI 410 martensitic stainless steel has not survived before. The use of diode lasers to increase the depth and width of hardness, as well as hardness uniformity in the hardened area, is considered as an effective challenge in other lasers, including the Nd:YAG laser, which was previously written by the authors of this paper. In this study, the effect of laser power, scanning speed and the stand-off distance (SOD) on the surface hardness and geometric dimensions of the hardened area of AISI 410 were studied by using diode laser. The microstructure changes of the steel surface were also measured and investigated. The microstructure of the hardened area was evaluated. Also, the microstructure and mechanical properties of furnace heat treatment were compared with the diode laser surface hardening. Figure 1 depicts the cross-section and geometrical responses of the hardened zone. The microstructure of the hardened area surveyed by an OM and FESEM device. MHD and the percentage of the ferrite phase in the structure investigated.

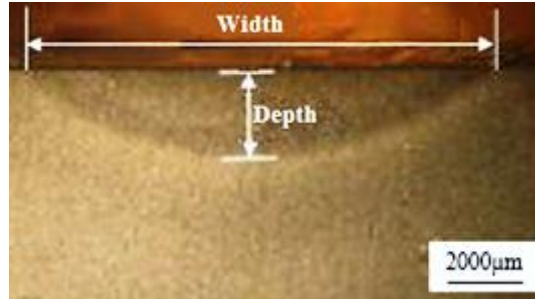


**Figure.1** Specimen cross-section and geometrical responses of the hardened zone.

## 2. Experimental work

The chemical composition of AISI 410 stainless steel used in this research is mentioned in [Table 1](#). The chemical composition measured by atomic spectroscopy. The specimens with (Specifications of the thickness =10 mm and the diameter = 65 mm) were selected.

**Table1** Chemical composition (Wt. %) of AISI 410

Element Name	C	Mo	Cr	Cu	S	P	Mn	Ni	Si	Al	V	Fe
Weight percent	0.15	0.03	13.5	0.11	0.024	0.018	0.51	0.12	0.28	0.008	0.021	Balance

In [Figure 2](#), the mechanism of the laser surface hardening process is depicted schematically. The laser stand-off distance or focal plane position is also shown in [Figure 2](#).

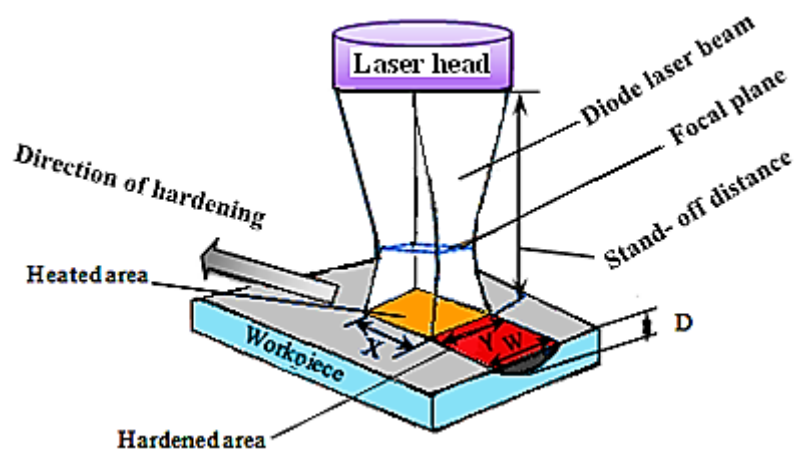


**Figure. 2** The schematic mechanism of the laser hardening process.

**Table. 2** Experimental layout and outcomes

Sample number	Input parameters			Output results					
	Scanning speed (mm/s)	stand-off distance (mm)	Laser power (W)	Maximum hardness (HV)	The depth of hardness (mm)	The width of hardness (mm)	MHD in depth	MHD in width	Ferrite percent (%)
1	5	65	1400	630	2.2	8.12	18813.71	28651.62	0.52
2	6	70	1200	490	1.4	8.42	12399.23	16417.13	1.92
3	4	70	1200	540	1.7	8.33	16211.64	21364.23	0.71
4	6	70	1600	620	1.8	8.21	18658.42	26621.61	0.62
5	7	65	1400	530	1.6	8.41	16053.43	20813.71	1.10
6	5	75	1400	520	1.5	8.52	15311.97	18355.25	1.50

A diode laser with a maximum power of 1600 W was used as a heat source for this research. Experimental settings and outcomes of laser hardening process by diode laser is shown in [Table 2](#). Scanning speed (4-7 mm/s), laser power (1200 – 1600 W), and stand-off distance (65-75 mm) were considered as input variables. [Table 3](#) shows the different dimensions of the incidence beam with a different focal plane position used in this research.

**Table 3** The relationship between the incident beam length, width, and area

Stand-off distance	Incident beam length (x)	Incident beam width (y)	Incident beam area (x-y)
65 mm	2.55 mm	9.94 mm	25.34 mm <sup>2</sup>
70 mm	3.60 mm	11.88 mm	42.77 mm <sup>2</sup>
75 mm	4.65 mm	13.82 mm	64.30 mm <sup>2</sup>

In [Figure 3](#), images of AISI 410 samples hardened by diode laser are shown. To investigate the microstructure of the hardened area, the samples are firstly cut into specific pieces and by mounting and metallurgical preparations they have been etched in the villa's reagent with a formula of ( Hcl 5cc, C6H3N3O7 2 gr, C2H5OH 100cc). Then, OM and FESEM Images are taken. Microhardness was accomplished by a micro-indentation device with a maximum load of 300 gr and a dwell time of 30 s. The geometric dimensions (depth and width) of the hardened area were obtained. [Figure 1](#) shows the depth and width of hardness as a macroscopic structure. The Precision measurement of hardened dimensions was done by ImageJ software. [Figure 4](#) illustrates the cross-sectional view of Vickers indenters in

depth and width of the hardened layer. The interval of the points in depth and width are  $100\mu\text{m}$  and  $300\mu\text{m}$ , respectively.

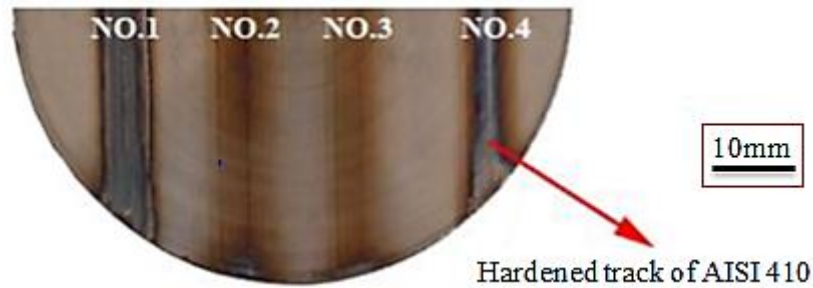


**Figure. 3** Image of the hardened laser samples (sample diameter is 65mm)

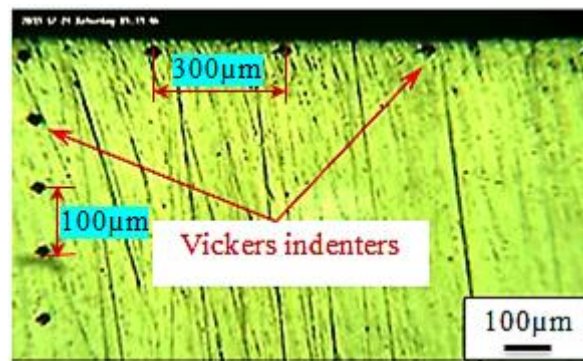


**Figure. 4** Image of Vickers indenters

### 3. Results and discussion

In this research, the effects of diode laser parameters (i.e., scanning speed, laser power, and stand-off distance) on AISI 410 martensitic stainless steel in surface hardening process was studied. To investigate the metallurgical properties, geometrical dimensions of the hardened area, microhardness distribution of the laser hardening, microstructure on the hardened surface, MHD and the percentage of the ferrite phase in the structure were analyzed.

#### 3.1 Micro-hardness distribution

Figure 5-a and 5-b show the micro-hardness changes from the surface to the depth and width of samples 1, 4 and 5.

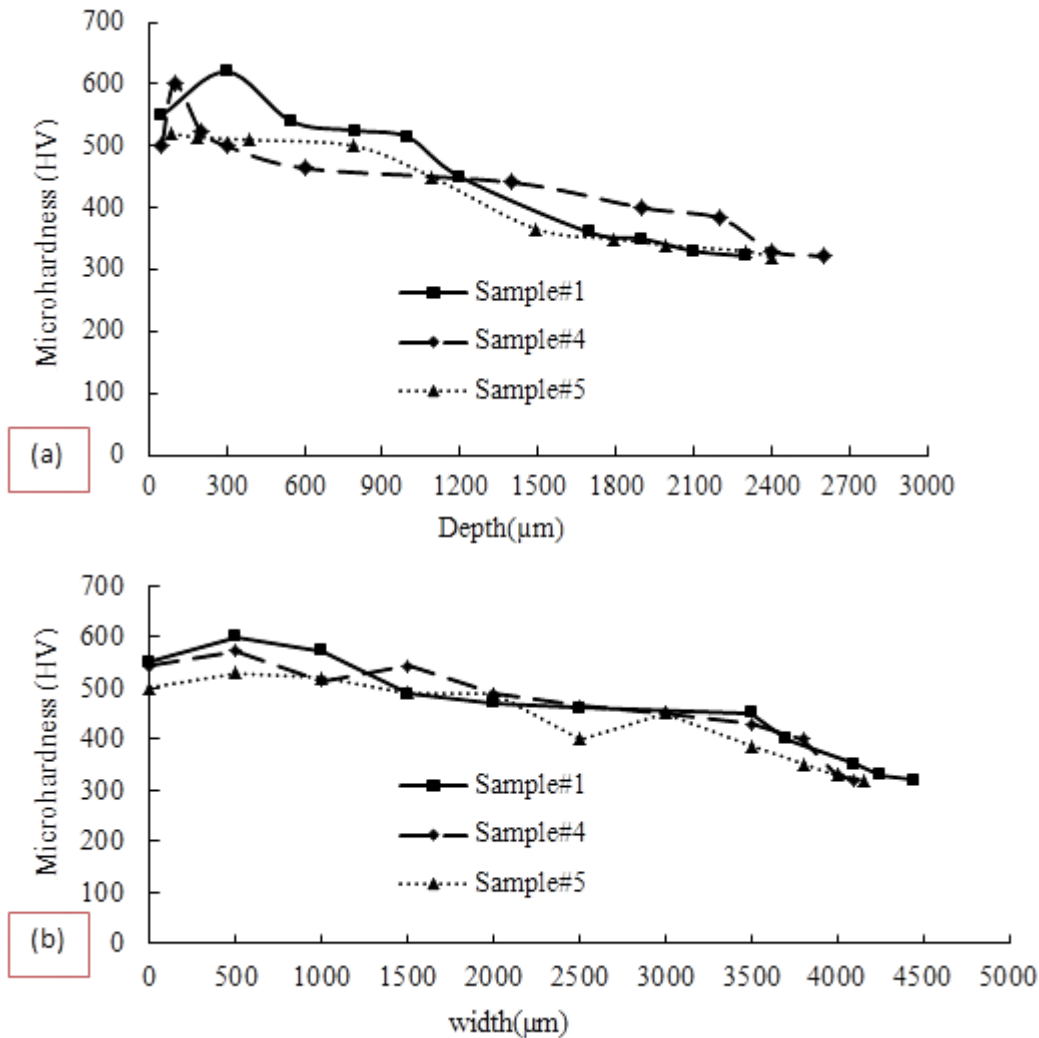


**Figure.5** Micro-hardness profile of the hardened layer in a) depth and b) width.

In [Figure 5-a](#) it is clear that surface hardness is increased and little by little is decreased along the depth of the hardened zone to reach the base metal hardness. It is because of the reduction of transferred laser energy in the material. Fine grain martensitic and ferrite phase dispersed in the hardened area. It is because of the high rate of quenching during laser hardening process, which produces unique metallurgical effects in the steel, such as improvement of microstructure and grain size, higher hardness with appropriate toughness in the steel. [Figure 5-b](#) depicts the microhardness distribution of the hardened layer in width. It is displayed in half of the width of the hardened zone. As it is clear, its distribution likes a sinusoidal function that in the hardness is the maximum in the center and decreases gradually in the outside of the hardened area. The reason for this phenomenon is the rectangular energy distribution of the laser beam that is illustrated in [Figure 6](#).

Figure 6-a and 6-b depict the images of the energy distribution in the diode laser beam and the shape of top-hat energy distribution, respectively [27]. Maximum surface hardness occurs in sample number 1 equal to 630 HV0.3 hardness. It means that the surface hardness increases 90% from 330 HV of the base metal.

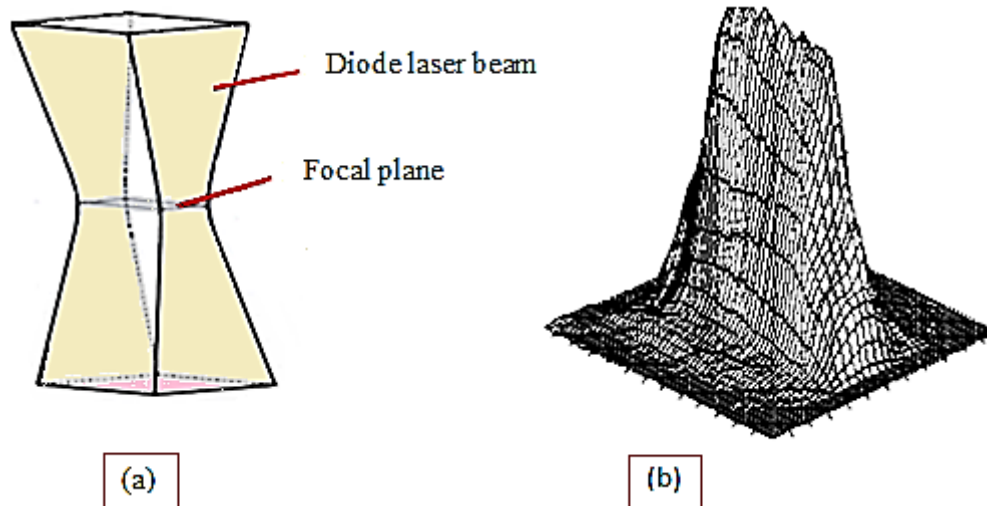


**Figure. 6** a) distribution of the diode laser beam energy, b) the shape of top-hat energy distribution [27-28].

To improve the results of the laser hardening process, the following parameters should be carefully considered:

1. The amount of heat entering the laser beam to the surface of the material.
1. The effect of metallurgical factors on the microstructure of the hardened area, such as grain size.

At first, the effect of heat input on the workpiece surface is studied. Equation 1 shows the laser heat input to the surface [29].

$$H = P / S \tag{1}$$

Therefore, by increasing the power of the laser beam and reducing the scanning speed on the workpiece, the heat input increases. Increases in the heat input lead to increases the hardness, while for Sample #1, Sample #4 and Sample #5 the heat input are 280 (j/mm), 266.6 (j/mm) and 200 (j/mm) respectively. The grain size of the laser hardened zone is an important issue for considering. The ASTM-112 standard is used to measure the grain size. To specify the grain size, the usual heat treatment cycle should be initiated at 850 ° C for one hour and then cooled at the furnace temperature. After achieved the declared heat treatment with a suitable

etching solution, the initial austenite particle, which is a solid solution of carbon and is stable at high temperatures is studied. Indeed, by measuring the size of the initial austenite, by using the Nital solution (2 ml Nitric acid and 98 ml Ethanol alcohol) the grain size is estimated [30]. For the base metal of the AISI 410, ASTM grain size number =7 (Equal to 30 $\mu$ m) reach to ASTM grain size number =11 (Equal to 7 $\mu$ m). By reducing the size of the initial austenitic grains, the structure is susceptible to the formation of a smaller martensitic phase during the process of austenite transformation into martensite. As the particle size of the martensite increases, the hardness of the surface of the hardened area increases. The Hall-Petch equation [30-31] presents the relationship between the size of the grain in the microstructure and the mechanical properties. Equation 2 describes Hall-Petch's relation:

$$\sigma_0 = \sigma_i + KD^{-1/2} \quad (2)$$

Where  $\sigma_i$  is yield stress,  $\sigma_0$  is the friction stress, K is the locking parameter and D is the mean diameter of the grain. Due to reduced grain size, the strength of the material and mechanical properties improve.

### 3.2 Geometrical dimensions of the hardened layer

As it is discussed above for Figure 6, the shape of the geometrical dimensions of the hardened zone is similar to the form of the laser energy distribution. By increasing the stand-off distance, the laser beam diverges, and the energy density is decreased, and a spot diameter of the laser becomes larger. In this paper increasing the stand-off distance (SOD) means getting away from The focal plane which is affected by penetration depth and also the hardness. Figure 7-a illustrates the effect of SOD on the distribution of the hardness in depth of the hardened zone. It is showed that in sample # 1 (SOD =65mm) the trend of hardness is higher than sample # 6 (SOD =75mm). The reason is that by decreasing the distance between the spot plane of the laser and workpiece, causes more energy induced in metal. It leads to increase the metallurgical transformation and causes more hardness. By focusing on the results presented in Table 2, it can understand that increasing the laser power causes increases in the depth of the hardened layer. More laser power leads to increases the austenitic temperature. So the micro-hardness and geometrical dimensions increases (compare samples # 4 and samples # 2). Figure 7-b illustrates the influence of the laser power on the hardness distribution in depth of the hardened layer. Scanning speed has a direct effect on the laser hardening results. Decreasing scanning speed increases the interaction time between the laser

beam and the workpiece. Therefore, heat input energy to the material increases which leads to increase the hardness and geometrical dimensions of the hardened layer.

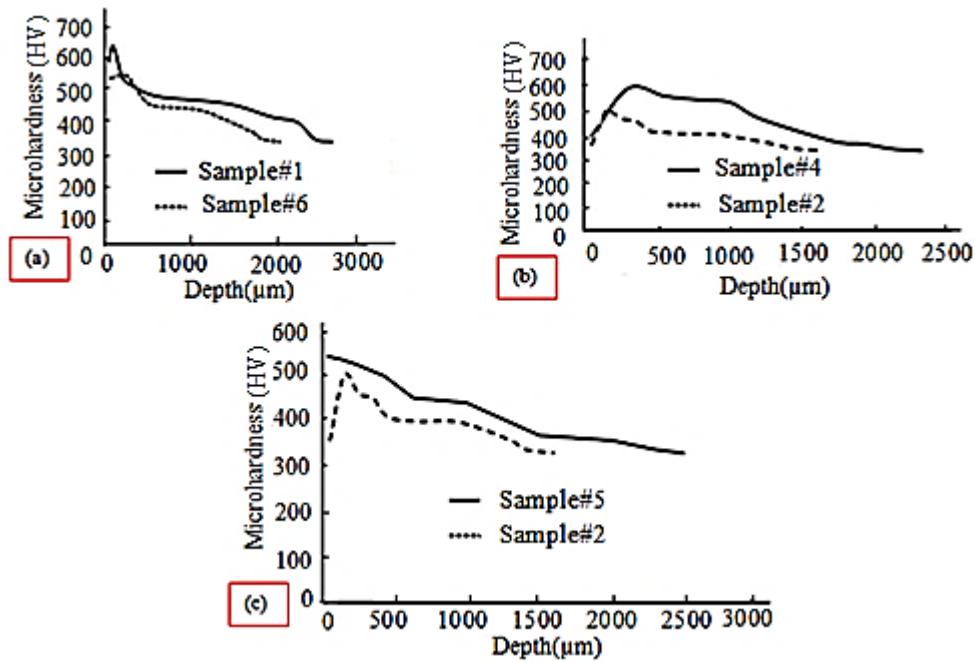


**Figure.7** Image of microhardness profile for Depth of the hardened area, a) effect of stand-off distance, b) effect of laser power, c) effect of scanning speed.

Influence of scanning speed could be seen in samples # 5 and samples # 2 (see [Table 2](#)). [Figure 7-c](#) illustrates the influence of scanning speed on the hardness distribution in depth of the hardened layer. In the following discussion, the influence of three other important parameters that have an important influence on the geometric dimensions is presented. These parameters are Beam density of the diode laser, the shape of the distribution of energy beam in diode laser and metallurgical properties such as the form of the phases in the microstructure, which is described below. The energy beam density of the diode laser is shown in [Equation 3](#) [3].

$$\text{Beam density} = \text{Laser power} / \text{Incident beam area} \quad (3)$$

By increasing the density of the energy beam, the surface temperature of the workpiece increases. Then the austenitic temperature rises, so hardness and the depth of the hardened area are increased. [Table 2](#) and [3](#) present the incident beam area and the laser power. By using [Equation 3](#), the beam density is calculated, for sample #1 and sample #6 as shown in [Figure 7-a](#), the beam densities are, 55.25 W/mm<sup>2</sup> and 21.77 W/mm<sup>2</sup>, respectively. Therefore, with more beam density in sample #1, the geometric dimensions (depth and width) of the hardened

area will be greater. According to [Figure 7-b](#), the beam density of sample #4 and sample #2 are  $37.40\text{W/mm}^2$  and  $28.05\text{ W/mm}^2$ , respectively. The reason for the increase in the geometric dimensions (of the hardened area) in sample #4, compared to sample #2, is the increase in the beam density of sample #4. In [Figure 7-c](#), both sample #5 and sample #2 have the same beam density, but because of increasing the heat input in sample #5 than sample #2 the geometric dimensions will be increased.

As shown in [Figure 6](#), the form of the energy distribution in the diode laser is rectangular. This top-hat distribution of energy leads to the expansion of the heat affected area, and the hardened area becomes larger, so the geometric dimensions of the hardened area are larger than another laser beams that are in the form of a gaussian distribution, such as (Nd:YAG laser and fiber laser). In addition when the shape of the particles is extended in the microstructure, the thermal conductivity and laser penetration increase, so the geometric dimensions of the hardened area increase. What is concluded from the microstructure images is that ferrite particles are stretched; therefore, the penetration of the thermal energy of diode laser in depth and width of the workpiece increases.

### **3.3 Microstructure of hardened layer**

To study the effect of laser hardening process on the microstructure of the material, the metallographic survey is performed by using optical microscopy (OM) and field emission scanning electron microscopy (FE-SEM). [Figures 8-a](#) and [8-b](#) show the microstructure of AISI 410 raw material by using OM and FE-SEM, respectively. It is seen that in its raw material ferrite is distributed in the martensitic field. It is obvious that there are several ferrite particles in the martensitic field.

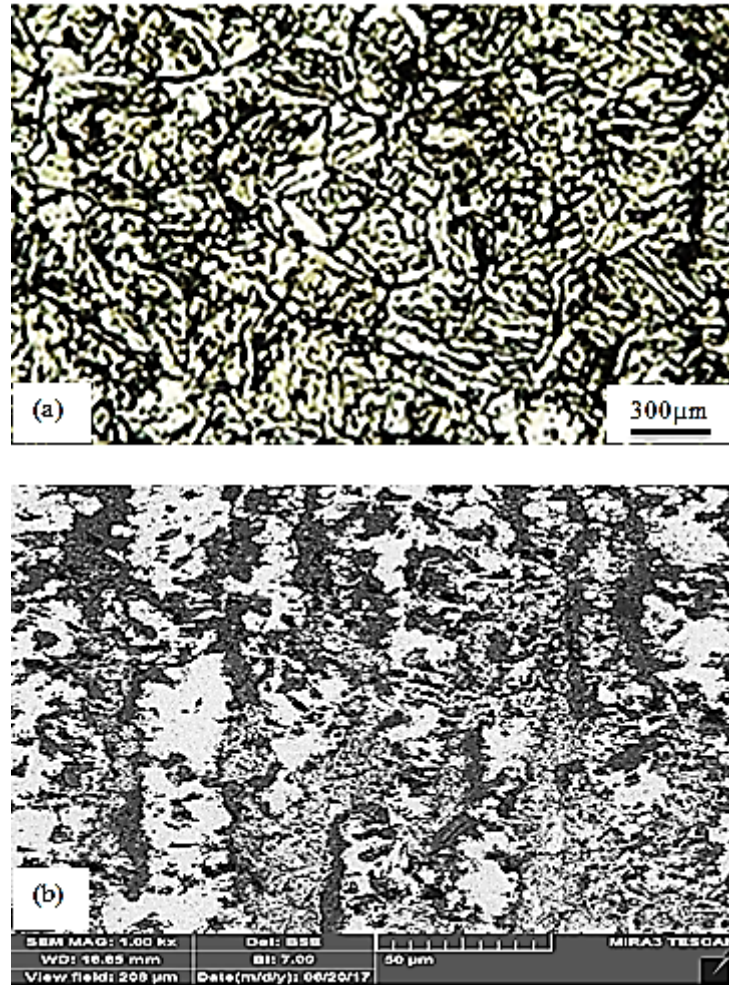


**Figure.8** Microstructure of AISI 410 raw material, a) OM, b) FESEM

Investigations show that when the heat input energy of the laser increases, (lower scanning speed, higher laser power, and lower SOD) austenite temperature for transformation phase increases and austenite grains became finer. Therefore, in this case, the ferrite phase percent decreases. By controlling the scanning speed, grains could be uniform. [Figures 9- a](#) and [9-b](#) show the microstructure of hardened layer of AISI 410 by using optical microscopy. It is observed that the figure of the ferrite is extended and finer in the microstructure. Consequently, in the laser hardening process by a diode laser, the hardness and geometric dimensions (depth and width) increase.

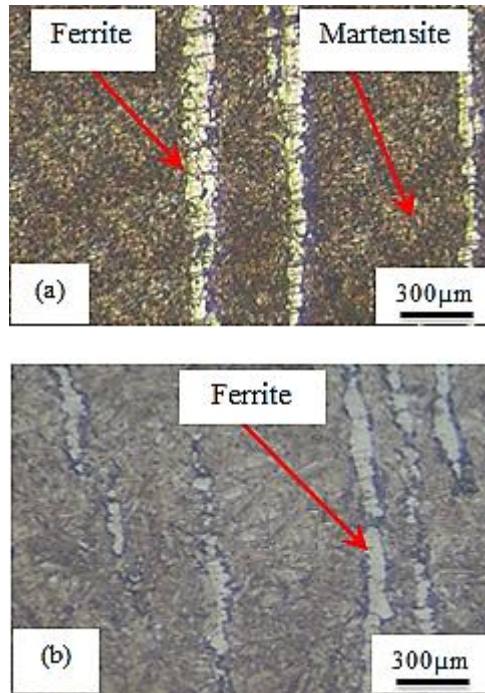


**Figure.9** The microstructure of AISI 410 laser hardened layer (OM), a) sample #1, b) sample#4

Figures 10-a and 10-b illustrate the microstructure of the hardened layer of Sample #1 and sample #4, respectively. These images are taken by using the FE-SEM. Due to higher laser energy, martensitic particles are finer, and ferrite particles are dissolved in the structure fields. Therefore, laser hardening has caused higher surface hardness, more uniform and suitable structure. It is observed that the ferrites are stretched and martensites are stretched and needle-shaped in the structure. Thus, laser hardening caused major changes in the size of the martensitic phase and the dissolution of the ferrites.

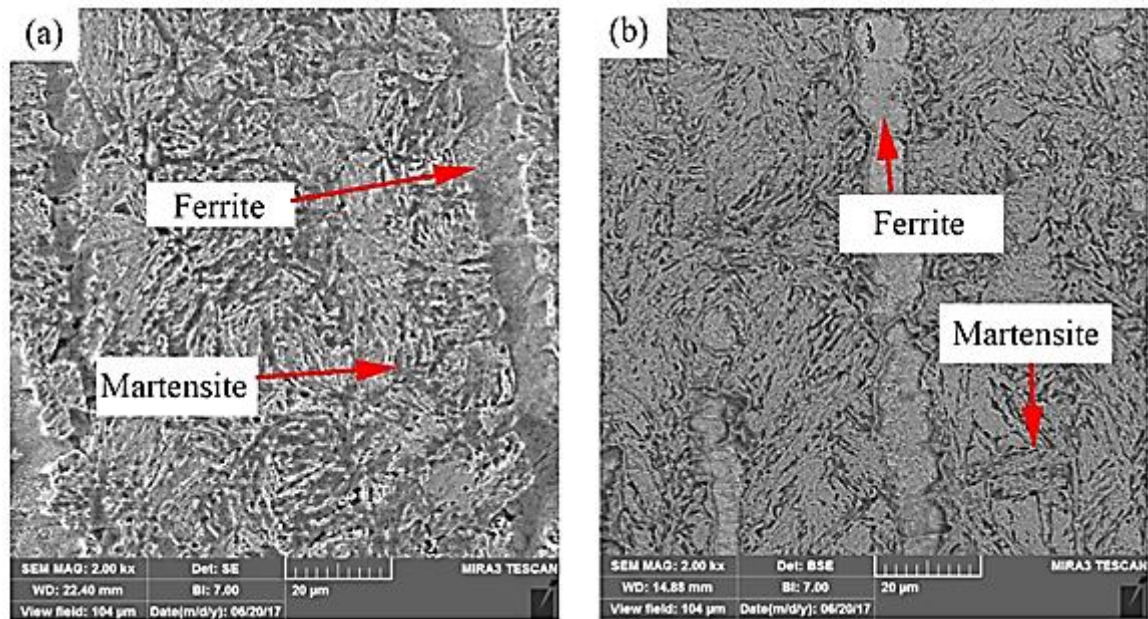


**Figure.10** The microstructure of AISI 410 laser hardened layer (FESEM), a) sample#1, b) sample #4

XRD spectra of raw material and laser-hardened area are shown in [Figure 11](#). By considering the XRD spectra, the martensite and ferrite phases are visible. Also, the ferrite and martensite particles of AISI 410 are smaller than raw material. Thus, XRD spectra confirm the hardness and geometric dimensions in the hardened area increase.

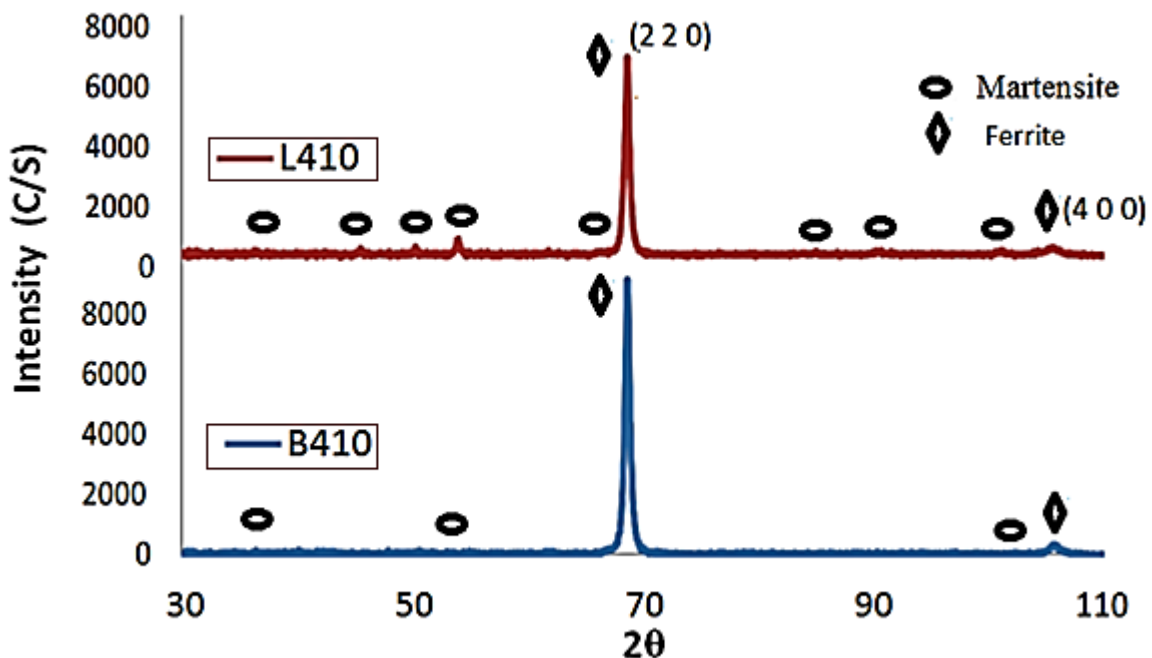


**Figure. 11** XRD spectra in the raw material (B410) and after the laser hardening (L410).

### 3.4 Microhardness deviation from the base metal (MHD)

To study how the microhardness distribution profile changes at the depth and width of the hardened area, the parameter of MHD is used according to [Equation 4 \[32\]](#).

$$\text{MHD} = \sum_{i=1}^n \frac{(X_i - X_{b,m})^2}{n} \quad (4)$$

Where  $X_i$  is the microhardness of point  $i$  and  $X_{b,m}$  is raw metal microhardness,  $n$  is the number of measured microhardness points. In the present research,  $n$  is 10 and  $X_{b,m}$  equal 330 wickers for AISI 410 stainless steel. Higher MHD in the laser hardening is more desirable. MHD is one of the most important output parameters in this study. Indeed, MHD designates the uniformity of hardness in the hardened area.

### 3.5 The percentage of the ferrite phase

By analyzing images of the microstructure using celemex software, the amount of ferrite phase particles in the structure of the hardened samples was obtained. The results are presented in [Table 2](#). The existence of ferrite in the hardened area reduces the hardness and strength of the steel. Microstructure images of the hardened surface were selected along the center of the hardened area. In [Figure 12-a](#) and [12- b](#) the red dots represent the ferrite phase and the blue field indicating martensites. As shown in [Table 2](#), in [Figure 12-a](#), the percentage of ferrite is lower than that of [Figure 12-b](#), The reason is that sample number #1 has a higher heat input energy (higher laser power and lower stand-off distance). Thus by increasing the laser thermal energy, the steel's austenitic temperature rises and the ferrites phases are solved in the structure. [Figure 13](#) depicts the relationship of ferrite percentage with the maximum surface hardness of samples. As seen, decreasing the ferrite percentage results in increasing the maximum surface hardness.

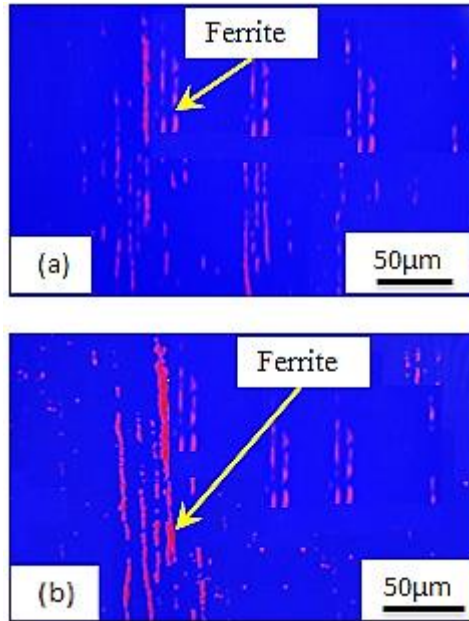


**Figure. 12** Determination of ferrite percentage by celemex software a) sample #1, b) sample #2

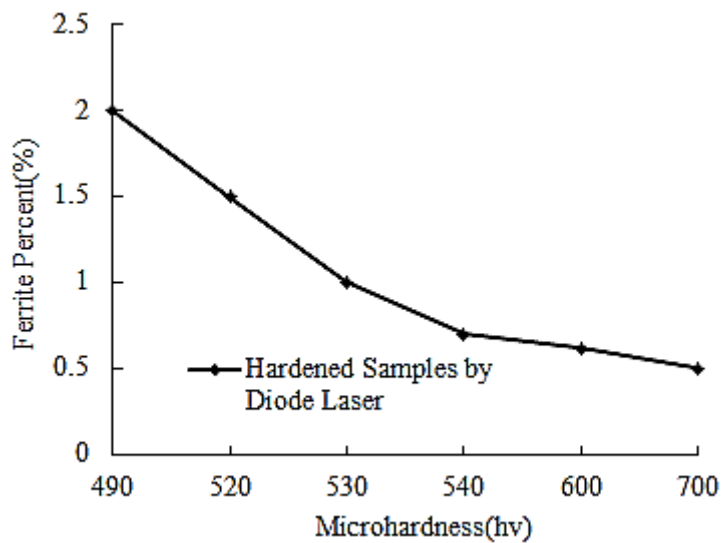


**Figure.13** Profile of ferrite percent in microhardness.

### 3.6 Comparison of the furnace hardening heat treatment (FHHT) and diode laser hardening (DLH)

In this section, FHHT was conducted to compare with the DLH method. For comparing the DLH with the conventional method, the furnace heat treatment according to the cycle presented in [Figure 14](#) was performed. The AISI 410 samples preheated to 540 ° C for 1 hour,

heated to 980 ° C with the rate of 70 ° C/hour, and were kept for 2 hours. Then samples quenched with three ways (air, oil, and water-cooling).

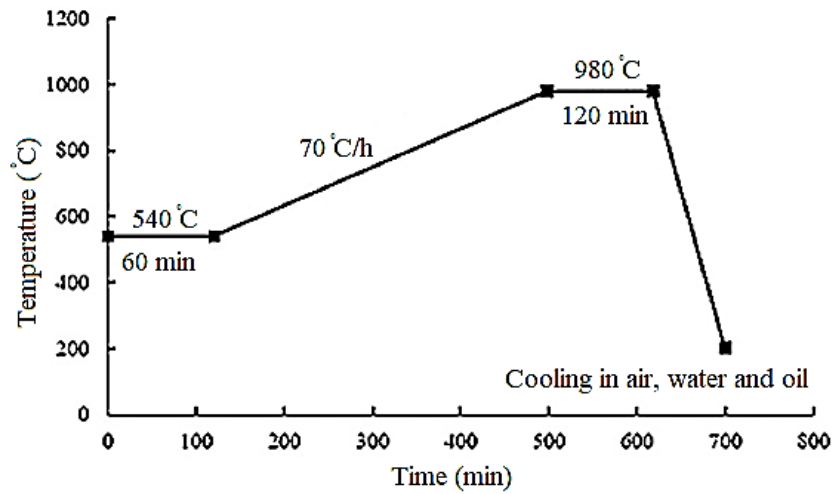


**Figure.14** Image of FHHT cycle for AISI 410 stainless steel [33].

### 3.6.1 Comparison of the hardness

Table 4 shows the comparison of the hardness results of furnace hardening heat treatment and laser surface hardening. As seen in Table 4 the hardness of furnace hardened of AISI 410 stainless steel quenched in the air, oil, and water are 412 Vickers, 434 Vickers, and 446 Vickers, respectively. Due to the possibility of micro crack formation in the water, and the lower the hardness in the air, the oil is an ideal quenching method with a hardness of 434 Vickers for AISI 410. So the hardness value with the diode laser hardening method (630 Vickers) is 1.4 times than the furnace hardening heat treatment.

**Table 4.** Comparison of furnace hardening heat treatment and laser hardening

Heat treatment cycle	furnace hardening heat treatment	laser hardening
Cooling in oil	434 Vickers	-
Cooling in water	446 Vickers	-
Cooling in air	412 Vickers	-
Self-cooling (Self- quenching)	-	630 Vickers

### 3.6.2 Comparison of the microstructure

As shown in Figure 15-a and 15-b the fine ferrites are dispersed in the rough martensitic field of FHHT samples, while in the DLH, these elements are interconnected in the fine martensitic field. Due to the high-energy concentration in the DLH, local hardness occurs,

while in the FHHT, the hardness is volumetric. The existence of ferrite in the martensite field reduces the hardness and strength of the steel. Because of small interaction time in the laser and high speed of the process, ferrites are detected in the martensite field. To reduce or remove them, increase the laser power and slow down the scanning speed could overcome this challenge. In FHHT technique because of keeping the sample at a specific time during the heating cycle, in the microstructure, fine ferrite and rough martensite phases are observed. Hence, in the FHHT technique the hardness increases, but this structure is brittle.

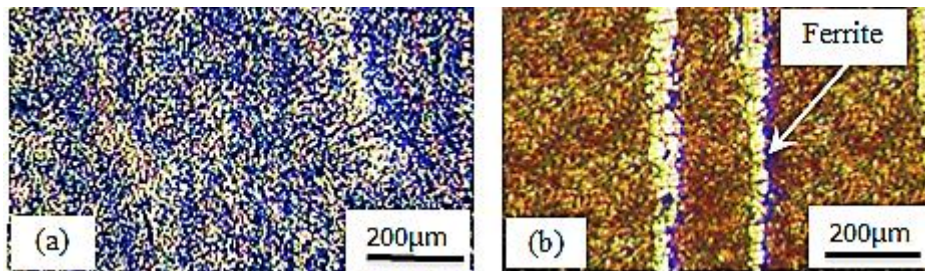


**Figure.15** Microstructure images of the hardened sample a) FHHT, oil quenched b) DLH, sample #1

### 3.6.3 Comparison of the impact test and fracture toughness

According to the heat treatment cycle of [Figure 14](#), AISI 410 is heated to 980 ° C, at this temperature the microstructure consists of austenite and ferrite, then, with the quenching operation, the sample is rapidly cooled, and the martensitic and ferrite particles are obtained with a very tough structure. Quenching operation creates internal stresses as well as brittle structures in steel. In this process, the hardness of the steel is higher, but the mechanical properties are reduced. To improve the mechanical properties of steel, such as an increase in toughness and a reduction in the residual stress after the quenching operation, the tempering heat treatment cycle is performed. The temperature and time selection of tempering operations depends on the chemical composition of the steel, the dimensions of the pieces and the mechanical properties are required. Tempering is performed by controlled heating of the quenched workpiece called the lower transformation temperature (Under the temperature of 723 ° C). This steel conducted relatively high hardness and strength after tempering at such high temperature of 600-700°C [33]. In the present study, to investigation of the hardness and toughness of The furnace heat treatment hardening samples, tempering sample with high temperatures of 650°C, tempering sample with a minimum of 250°C [34] and No tempering

sample, compared to the laser hardened sample were accomplished. Toughness properties by impact test (according to ASTM-A370 standard at ambient temperature) , and microstructure analysis has been evaluated. Charpy impact tests at ambient temperature and amount of energy absorbed by studied structures with dimensions of 10 mm × 10 mm × 55 mm and with V-notch to a depth of 2 mm during fracture was conducted. (see [Table 5](#)). The results showed that hardness of the samples at 250 ° C and 650 ° C, reached 412 HV and 380 HV, respectively. In addition The results of the impact test on the furnace heat treatment samples at the tempering setup of 250 ° C and 650 ° C, reached 12 J and 22 J, respectively. Thus, in furnace heat treatment samples, if the tempering operation is carried out at 650 ° C, the hardness will be reduced to 380 HV while the toughness will be better. By tempering operation at 250 ° C, the hardness will reach to 412 HV but the steel will be quite brittle. The impact test was also performed on the best laser surface hardening sample of AISI 410 (sample #1).

**Table 5** Comparison of the hardness and impact test at 25 ° C (ambient temperature) and fracture toughness of the FHHT and DLH methods.

Type of operation	Base metal	Furnace heat treatment, oil quenched without tempering operation	Furnace heat treatment, oil quenched with tempering operation at 250 ° C	Furnace heat treatment, oil quenched with tempering operation at 650 ° C	Diode laser hardening by Self-quenching
Hardness (HV)	336	434	412	380	630
Impact energy (J)	15	10	12	22	35
Fracture toughness $k_{1c}(MP\sqrt{m})$	51.31	37.85	43.40	68.38	96.87

About the impact energy values, [Equation 5](#) describes the fracture toughness [\[35\]](#):

$$K_{1c}^2 = 0.22E \times (CVN)^{1.5} \quad (5)$$

Where  $k_{1c}$  the fracture toughness in the plane strain states, E is Young's modulus, and CVN is the impact energy of the V-notch sample in the Charpy impact test, fracture toughness is a

property, which describes the ability of a material to resist fracture, and is one of the most important properties of any material for many design applications. Fracture toughness is a quantitative way of expressing a material's resistance to brittle fracture when a crack is present. A material with high fracture toughness may undergo ductile fracture as opposed to brittle fracture. According to [Table 5](#), the result shows that diode laser hardening has higher hardness and toughness than furnace hardening heat treatment. Having a higher hardness and higher fracture toughness at the same time in laser surface hardening could improve the application of this process, which could have so many applications in industries such as steam turbine blade application. [Figure 16-a, b and c](#) show images of the microstructure of tempering operation at 250°C and 650°C and diode laser hardening respectively. Fine particles of ferrite and martensite exist in the structure of the tempered at 250°C, which causes higher hardness and lower fracture toughness (See [Figure 16-a](#)). **As shown in [Figure 16-b](#), in the tempered state at 650°C, the coarse ferrite and martensite particles has been scattered in the microstructure, this can be lead to lower hardness and higher fracture toughness in the AISI 410 hardened sample.** In the diode laser hardening, as shown in [Figure 16-c](#), finer particles of ferrite and martensite can be seen which causes higher hardness and higher fracture toughness.

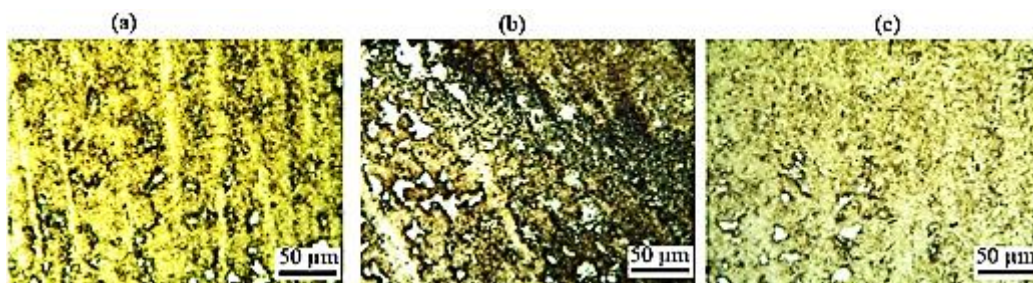


**Figure.16** Microstructure images of the tempering operation at a) 250°C b) 650°C  
c) Diode laser hardening

#### 4. Conclusions

The influences of diode laser parameters (i.e., laser power, scanning speed, and stand-off distance) on AISI 410 martensitic stainless steel in surface transformation hardening process was studied. Geometrical dimensions of the hardened layer, microhardness distribution in depth and width of laser hardening and microstructure on the hardened surface were analyzed. The following conclusions can be drawn:

1. Increasing the laser power and reducing scanning speed, (increasing heat input), lead to increases in microhardness and depth of the hardened layer. Decreasing the

stand-off distance causes more energy induced to the material. Regarding rectangular energy distribution of the laser beam, hardness, and depth of the hardening layer increases.

2. The maximum surface hardness of 630 HV0.3 with the maximum depth of the hardened layer of 2.2 mm is obtained. It means that the surface hardness increases 90% from 330 HV of the base metal.
3. The microhardness deviation (MHD) specifies the uniformity of hardness in the hardened area, so, if the hardness decreases gradually from surface to depth, the MHD in depth will be higher.
4. To reduce or eliminate ferrite phases, the lower scanning speed and the higher laser power is recommended. Also in the laser hardening, ferrite particles are interconnected in the microstructure. However, in the furnace hardening operation, are finer and more dispersed.
5. The hardness value of the diode laser hardening method (630 HV0.3) is 1.4 times than furnace hardening heat treatment.
6. The maximum hardness and impact energy values for the laser hardened samples are 630 HV and 35 J, respectively. While these values for the furnace heat treatment sample are 380 HV and 35 J, respectively.

## 5. References:

1. E. Kannatey, Jr. Asibu, Principles of Laser Materials Processing, Second Edition, pp. 568-581, New Jersey: John Wiley and Sons, 2009.
2. M. Moradi, M. Karami Moghadam, M. Kazazi, Improved Laser Surface Hardening of AISI 4130 Low Alloy Steel with Electrophoretically Deposited Carbon Coating, Optik, Vol. 178 (February), pp. 614-622, 2019.
3. M. Moradi, M. Karami Moghadam, High power diode laser surface hardening of AISI 4130; statistical modeling and optimization, Optics & Laser Technology Vol. 111 (April), pp.554-570, 2019.
4. A Khorram, A Jafari, M Moradi, Effect of Linear Heat Input on the Morphology and Mechanical Properties of Ti-6Al-4V Welded Using a CO<sub>2</sub> Laser, Lasers in Engineering, Vol 40 (1-3), pp. 49-64, 2018.

5. A. H. Faraji, M. Moradi, M. Goodarzi, P. Colucci, Carmine Maletta. An investigation on the capability of hybrid Nd:YAG laser-TIG welding technology for AA2198 Al-Li alloy. *Optics and Lasers in Engineering*, Vol. 96, PP.1-6. 2017.
6. A. Khorram, A. Jafari, M. Moradi. Laser brazing of 321 and 410 stainless steels using BNI-2 nickel-based filler metal. *Modares Mechanical Engineering*, Vol.17 No. 1, pp. 129-135, 2017.
7. M. Moradi, M. Ghoreishi and A. Khorram. Process and Outcome Comparison between Laser, Tungsten Inert Gas (TIG) and Laser-TIG Hybrid Welding. *Journal of Lasers in Engineering*, Vol 39, No. 3-6, pp. 379-391. 2018.
8. M. Moradi, A. Mohazabpak. Statistical modeling and optimization of laser percussion micro-drilling on Inconel 718 sheet using response surface methodology. *Journal of Lasers in Engineering*, Vol 39, No. 4-6, pp. 313-331, 2018.
9. M. Moradi, Omid Mehrabi, Taher Azdast, Khaled Y. Benyounis, Enhancement of low power CO<sub>2</sub> laser cutting process for injection molded polycarbonate, *Optics & Laser Technology*, Vol. 96C, pp. 208–218, 2017.
10. L. Li, “The advances and characteristics of high-power diode laser materials processing”, *Optics and Lasers in Engineering* 34, pp. 231-253, 2000.
11. R. Puli, G. D. Janaki Ram, Wear and corrosion performance of AISI 410 martensitic stainless steel coatings produced using friction surfacing and manual metal arc welding, *Surface and Coatings Technology*, Vol. 209, No. 24, pp. 1-7, 2012.
12. B. Mahmoudi, A. R. Sabour Aghdam, M. J. Torkamany, Controlled laser transformation hardening of martensitic stainless steel by pulsed Nd: YAG laser, *Electronic Science and Technology*, Vol. 8, No. 01, pp. 87-90, 2010.
13. R. Li, Y. Jin, Zh. Li, K. Qi, A comparative study of high-power diode laser and CO<sub>2</sub> laser surface hardening of AISI 1045 steel, *Materials Engineering and Performance*, Vol. 23, No. 09, pp. 3085-3091, 2014.
14. S. Guarino, M. Barletta, A. Afilal, High Power Diode Laser (HPDL) surface hardening of low carbon steel: Fatigue life improvement analysis, *Journal of Manufacturing Processes*, Vol 28, No.01, pp. 266-271, 2017.
15. O. Netprasert, V. Tangwarodomnukun, Ch. Dumkum, Surface Hardening of AISI 420 stainless Steel by Using a Nanosecond Pulse Laser, *Materials Science Forum*, Vol. 911, pp. 44-48, 2018.

16. O.Yazici, S.Yilmaz, Investigation of effect of various processing temperatures on abrasive wear behaviour of high power diode laser treated R260 grade rail steels, *tribology International*, Vol 119, pp. 222-229, 2018.
17. D. A. Lesyk, S. Martinez, B. N. Mordyuk, V. V. Dzhemelinskyi, Lamikiz, G. I. Prokopenko, K. E. Grinkevych, I. V. Tkachenko, Laser-Hardened and Ultrasonically Peened Surface Layers on Tool Steel AISI D2: Correlation of the Bearing Curves' Parameters, Hardness and Wear, *Journal of Materials Engineering and Performance*, Vol 27, No 02, pp. 764–776, 2018.
18. B.Syed, S.M. Shariff, G.Padmanabham, Sh.Lenka, B.Bhattacharya, S .Kundu, Influence of laser surface hardened layer on mechanical properties of re-engineered low carbon steel sheet, *Materials Science and Engineering: A*, Vol 685, pp. 168-177, 2017.
19. N.Barka, J.Brousseau, Case study of laser hardening process applied to 4340 steel cylindrical specimens using simulation and experimental validation, *Case Studies in Thermal Engineering*, Vol.11, pp. 15-25, 2018.
20. G. Telasang, J. D. Majumdar, G. Padmanabham, I. Manna, Wear and corrosion behavior of laser surface engineered AISI H13 hot-working tool steel, *Surface and Coatings Technology*, Vol. 261, No. 01, pp. 69-78, 2015.
21. A. Fahdil iidan, O. Akimov, L.Golovco, O.Goncharuk, K.Kostyk, The study of the influence of laser hardening conditions on the change in properties of steel. *Iadn*; 2(5), pp. 69-73, 2016.
22. Sh. Safdar, L. Li, M.A. Sheikh, M.J .Schmidt. Modelling the effect of laser beam geometry on laser surface heating of metallic materials. *Proceedings of the 23 International Congress on Applications of Lasers and Electro-Optics*, 2004.
23. M. Moradi, M. KaramiMoghadam, J. Zarei, B. Ganji. The effects of gha laser pulse energy and focal point position on laser surface hardening of AISI 410 stainless steel. *Modares Mechanical Engineering*. 17(7), pp. 311-318. 2017.
24. S.A. Jenabali Jahromi, A. Khajeh, B. Mahmoudi. Effect of different pre-heat treatment processes on the hardness of AISI 410 martensitic stainless steels surface-treated using pulsed neodymium-doped yttrium aluminum garnet laser. *Materials and Design*, 34, pp. 857–862, 2012.

25. P. Sun, Sh. Li, G. Yu, X. He, C. Zheng & W. Ning, “Laser surface hardening of 42CrMo cast steel for obtaining a wide and uniform hardened layer by shaped beams”, *Int J Adv Manuf Technol*, Vol. 70, pp.787–796. 2014.
26. B. Ehlers, H.J. Herfurth, S. Heinemann, Hardening and welding with high power diode lasers, *Proc. SPIE 3945*, pp. 63–70. 2000.
27. R. Li, Y. Jin, Zh. Li, & K. Qi, A Comparative Study of High-Power Diode Laser and CO<sub>2</sub> Laser Surface Hardening of AISI 1045 Steel, *JMEPEG*, Vol. 23, pp. 3085–3091, 2014.
28. M. Moradi, M.M. Fallah, S. Jamshidi Nasab, Experimental study of surface hardening of AISI 420 martensitic stainless steel using high power diode laser, *Transaction of the Indian institute of metal*, Springer Nature, pp.1-18, 2018.
29. E. Haddadi, M. Moradi, A. Karimzad Ghavidel, A. Karimzad Ghavidel, S. Meiabadi. *Experimental and Parametric Evaluation of Cut Quality Characteristics in CO<sub>2</sub> Laser Cutting of Polystyrene*, *Optik*, Vol. 184, pp. 103-114, 2019.
30. B.Jung a, H.Lee b, H.Park, Effect of grain size on the indentation hardness for polycrystalline materials by the modified strain gradient theory, *International Journal of Solids and Structures* Vol 50, pp. 2719–2724, 2013.
31. X.Liu, F.Yuan, Y.Weii, Grain size effect on the hardness of nanocrystal measured by the Nano- size indenter, *Applied Surface Science* Vol 279, pp. 159-166, 2013.
32. M. R. Jelokhani-Niaraki, N. B. Mostafa Arab, H. Naffakh-Moosavy, & M. Ghoreishi, The systematic parameter optimization in the Nd:YAG laser beam welding of Inconel 625, *The International Journal of Advanced Manufacturing Technology*. Vol. 84, NO 9–12, pp. 2537–2546, (June) 2016.
33. M. Moradi, M. Fallah, S. Jamshidi Nasab, Experimental study of surface hardening of AISI 420 martensitic stainless steel using high power diode laser. *Transaction of the Indian institute of metal: Springer Nature*. Vol. 71 (8), pp. 1-18, 2018.
34. M Moradi, H Arabi, S Jamshidi Nasab, KY Benyounis. A comparative study of laser surface hardening of AISI 410 and 420 martensitic stainless steels by using diode laser. *Optics and Laser Technology*, 111, pp. 347-357, (April) 2019.
35. A. Salemi Golezani, The Effect of Microstructure on Estimation of the Fracture Toughness (KIC) Rotor Steel Using Charpy Absorbed Energy (CVN), *Journal of Advanced Materials and Processing*, Vol. 1, No. 3, pp. 11-17, 2013.